J|A|C|S
ARTICLES

Published on Web 05/21/2009

FerriBRIGHT: A Rationally Designed Fluorescent Probe for Redox Active Metals

Daniel P. Kennedy, Chad M. Kormos, and Shawn C. Burdette*

Department of Chemisty, University of Connecticut, 55 North Eagleville Road, U-3060, Storrs, Connecticut 06269

Received March 3, 2009; E-mail: shawn.burdette@uconn.edu

Abstract: The novel catechol−BODIPY dyad, 8-(3,4-dihydroxyphenyl)-2,6-bis(ethoxycarbonyl)-1,3,5,7-tetramethyl-4,4-difluoro-4-bora-3a,4a-diaza-*s*-indacene (FerriBRIGHT) was rationally designed with the aid of computational methods. FerriBRIGHT could be prepared by standard one-pot synthesis of BODIPY fluorophores from 3,4-bis(benzyloxy)benzaldehyde (**1**) and 3,5-dimethyl-4-(ethoxycarbonyl)pyrrole (**3**); however, isolating the dipyrrin intermediate 8-[3,4-bis(benzyloxy)phenyl]-2,6-bis(ethoxycarbonyl)-1,3,5,7-tetramethyl-4,4-diaza-*s*-indacene (**7**) prior to reaction with excess $BF_3 \cdot OEt_2$ led to marked improvements in the isolated overall yield of the desired compound. In addition to these improvements in fluorophore synthesis, microwave-assisted palladium-catalyzed hydrogenolysis of benzyl ethers was used to reduce reaction times and catalyst loading in preparation of the desired compound. When FerriBRIGHT is exposed to excess $FeCl_3$, $CuCl_2$, $[Co(NH_3)_5Cl]Cl_2$, 2,3-dichloro-5,6-dicyanobenzoquinone, or ceric ammonium nitrate in methanol, a significant enhancement of fluorescence is observed. FerriBRIGHT-Q, the product resulting from the oxidation of the pendant catechol to the corresponding quinone, was found to be the emissive species. FerriBRIGHT-Q was synthesized independently, isolated, and fully characterized to allow for direct comparison with the spectroscopic data acquired in solution. Biologically relevant reactive oxygen species, such as H_2O_2, $^{\bullet}OH$, $^1O_2$, $O_2^{\bullet-}$, and bleach (NaOCl), failed to cause any changes in the emission intensity of FerriBRIGHT. In accordance with the quantum mechanical calculations, the quantum yield of fluorescence for FerriBRIGHT ($\Phi_{fl} \approx 0$) and FerriBRIGHT-Q ($\Phi_{fl} = 0.026$, $\lambda_{ex}/\lambda_{em} = 490$ nm/510 nm) suggests that photoinduced electron transfer between the catechol and the BODIPY dye is attenuated upon oxidation, which results in fluorescence enhancement. Binding studies of FerriBRIGHT with $Ga(NO_3)_3$, a redox-inactive analogue of Fe(III), provided conditional binding constant $\log \beta_{12}' = 13.3 \pm 0.2$ for a $[Ga(FerriBRIGHT)_2]^-$ complex. A 2.8-fold enhancement of fluorescence intensity upon addition of Ga(III) to FerriBRIGHT suggests the possibility of metal ion sensing with this new class of compounds.

Introduction

Iron and copper participate in numerous crucial biological functions, but both metal ions also have been implicated in chemistry detrimental to cellular health. Ferrous iron reduces hydrogen peroxide (H_2O_2) to hydroxyl radicals ($^{\bullet}OH$) and hydroxide by the Fenton reaction.[1] Reduction of ferric iron by H_2O_2 can both initiate this chemistry and be catalytically recycled to generate these harmful reactive oxygen species (ROS). Analogous redox cycles between copper and H_2O_2 also produce ROS. Although cells have mechanisms for deactivating ROS, loss of iron or copper homeostasis may overwhelm the cells' capacity to process such species.[2] Reactions of ROS with lipids, proteins, or nucleic acids can lead to gene mutations or other irreversible cell damage;[3] however, only limited, circumstantial evidence links ROS formation directly to iron or copper homeostasis. For example, postmortem examinations of brain tissues from patients suffering from Alzheimer's[4] and Parkinson's[5] disease reveal a marked increase in metal accumulation in comparison to tissues from healthy subjects, which has led to the hypothesis that compromised metal ion trafficking and subsequent ROS formation are part of the disease pathology.

Studying loosely bound transition-metal ions in biology remains difficult because of the lack of fluorescent sensors that exhibit turn-on behavior. The majority of the existing sensors for redox-inert metal ions such as Ca^{2+} and Zn^{2+} utilize photoinduced electron transfer (PeT) as the signaling mechanism.[6] In contrast, there are very few examples of sensors that utilize similar strategies to achieve turn-on sensing for Fe^{3+},[7] and the majority of PeT iron sensors utilize fluorescence

(1) Haber, F.; Weiss, J. *Proc. R. Soc. London, Ser. A.* **1935**, *147*, 332–351.
(2) Papanikolaou, G.; Pantopoulos, K. *Toxicol. Appl. Pharmacol.* **2005**, *202*, 199–211.
(3) Zhang, Z. H.; Wei, T. T.; Hou, J. W.; Li, G. S.; Yu, S. Z.; Xin, W. J. *Eur. J. Pharmacol.* **2003**, *467*, 41–47.
(4) Bartzokis, G.; Sultzer, D.; Mintz, J.; Holt, L. E.; Marx, P.; Phelan, C. K.; Marder, S. R. *Biol. Psychiatry* **1994**, *35*, 480–487.
(5) Dexter, D. T.; Wells, F. R.; Lee, A. J.; Agid, F.; Agid, Y.; Jenner, P.; Marsden, C. D. *J. Neurochem.* **1989**, *52*, 1830–1836.
(6) de Silva, A. P.; Gunaratne, H. Q. N.; Gunnlaugsson, T.; Huxley, A. J.; McCoy, C. P.; Rademacher, J. T.; Rice, T. E. *Chem. Rev.* **1997**, *97*, 1515–1566.
(7) Bricks, J. L.; Kovalchuk, A.; Trieflinger, C.; Nofz, M.; Buschel, M.; Tolmachev, A. I.; Daub, J.; Rurack, K. *J. Am. Chem. Soc.* **2005**, *127*, 13522–13529.

10.1021/ja901653u CCC: $40.75

quenching as the signaling mechanism.[8−10] In PeT systems, electrons on receptor ligands quench the excited state of the fluorophore, and subsequent coordination of a metal ion to the receptor prevents these electrons from participating in the quenching process. Unlike closed-shell metal ions, Fe^{3+} (d^5) has additional metal-centered electrons, orbitals, and charge-transfer bands that can provide nonradiative decay pathways for the excited state of fluorophores. While methodologies for constructing fluorescent sensors for redox-inert metals are well developed, designing useful sensors for transition metals presents a significant challenge.

Several efforts to achieve turn-on behavior in transition-metal ion sensing have been reported. These sensors utilize several mechanisms to achieve emission enhancement including fluorophore isomerization,[11,12] exciplex formation,[13] and shifts in excitation wavelength.[14,15] While these approaches are noteworthy, there are several drawbacks. Fluorophore isomerization is often irreversible under the conditions in which the sensors are employed, so measuring concentration changes is impossible. Exciplex formation requires significant ligand design considerations. Recently, a fluorescent dosimeter for Fe^{3+} that operated by a ligand oxidation process was reported; however, only a few of the oxidation products responsible for the emission increase could be fully characterized.[16]

On the basis of experimental results on PeT switching systems using 3,3′,5,5′-tetramethylboron dipyrromethene (BODIPY) fluorophores,[17,18] we reasoned that catechol could quench the emission of some BODIPY derivatives. A subsequent two-electron oxidation of the catechol to the quinone would yield a fluorescent species. Fe(III), which readily oxidizes catechol, is the likely precursor of Fe(II) required to initiate Fenton chemistry and the end product of the reaction sequence. Intercepting Fe(III) therefore would be a useful metric for ascertaining levels of oxidative stress. Such a redox-mediated fluorescence response could circumvent metal-based quenching pathways and be a paradigm for a new generation of fluorescent probes for transition-metal ions.

Experimental Section

General Procedures. All the materials listed below were of research grade or spectrograde in the highest purity commercially available from Acros Organics or TCI America. Dichloromethane (CH_2Cl_2), toluene ($C_6H_5CH_3$), and tetrahydrofuran (THF) were sparged with argon and dried by passage through a Seca solvent purification system. All chromatography and TLC were performed on silica (230−400 mesh) from Silicycle unless otherwise specified. Activated basic alumina (∼150 mesh) was obtained from Acros Organics. Thin-layer chromatograms were developed with mixtures of ethyl acetate (EtOAc)/hexanes or CH_2Cl_2/methanol (MeOH) unless otherwise specified and were visualized with 254 and 365 nm light and I_2 or Br_2 vapor. ^{1}H and ^{13}C NMR spectra were recorded using a Bruker 400 MHz NMR instrument, and chemical shifts are reported in parts per million on the δ scale relative to the peak for tetramethylsilane. IR spectra were recorded on a Nicolet 205 FT-IR instrument, and the samples were prepared as KBr pellets. High-resolution mass spectra were recorded at the University of Connecticut mass spectrometry facility using a micromass Q-Tof-2 mass spectrometer operating in positive ion mode. The instrument was calibrated with Glu-fibrinopeptide B, 10 pmol/μL, using a 50:50 solution of acetonitrile (CH_3CN) and H_2O with 0.1% acetic acid (AcOH).

2-(*tert*-Butoxycarbonyl)-3,5-dimethyl-4-(ethoxycarbonyl)pyrrole (3a). To a chilled mixture of *tert*-butyl acetoacetate (15.8 g, 100 mmol) and glacial acetic acid (20 mL) was slowly added a 50% (w/v) aqueous solution of $NaNO_2$ (6.90 g, 100 mmol). The temperature of the mixture was maintained between 2 and 5 °C throughout the addition. The resulting solution was warmed to 23 °C and allowed to stand for 4 h. A solution of ethyl acetoacetate (13.0 g, 100 mmol) in glacial acetic acid (40 mL) was added in one portion to the mixture and the resulting solution warmed to 65 °C with an oil bath. To the warm solution was added zinc dust (6.54 g, 100 mmol) in small portions. Another portion of zinc dust was added after the initial effervescence subsided (2 g, 30 mmol). The mixture was maintained at 65−70 °C for 1 h and then poured into 600 mL of cold water. The resulting precipitate was isolated via filtration and dried under vacuum to afford a pale yellow solid (13.6 g, 50.9%). The product was recrystallized from MeOH: TLC $R_f = 0.64$ (1:1 hexanes/EtOAc); mp 131−133 °C; ^{1}H NMR (400 MHz, $CDCl_3$) δ 9.10 (s, 1H, NH), 4.27 (q, $J = 7.2$ Hz, 2H, CH_2CH_3), 2.52 (s, 3H, CH_3), 2.49 (s, 3H, CH_3), 1.56 (s, 9H, *t*-Bu), 1.33 (t, $J = 7.2$ Hz, 3H, CH_2CH_3); ^{13}C NMR (100 MHz, $CDCl_3$) δ 165.6, 161.2, 138.3, 130.0, 119.2, 113.4, 81.2, 59.4, 28.5, 14.4, 14.3, 12.0; IR (KBr pellet) 3303, 2980−2910, 1702, 1656 cm^{-1}; HRMS (+ESI) *m*/*z* calcd for MH^+ 268.1549, found 268.1382.

3,5-Dimethyl-4-(ethoxycarbonyl)pyrrole (3). To a vigorously stirred suspension of **3a** (6.50 g, 24.3 mmol) in absolute EtOH (20 mL) was added 10 N HCl (9.1 mL) in one portion. The resulting heterogeneous mixture was heated to 65 °C for 1 h to provide an orange solution. Effervescence was observed when the solution temperature reached 55−60 °C. The resulting solution was cooled to 2−4 °C and diluted with 80 mL of water to provide an orange oil that solidified upon standing at 5 °C. A light pink crystalline precipitate was isolated by filtration and washed with water. The solids were dried under vacuum to afford the product as a salmon pink powder (3.62 g, 89.0%). The product was recrystallized from hexanes: TLC $R_f = 0.55$ (1:1 hexanes/EtOAc); mp 72−74 °C; ^{1}H NMR (400 MHz, $CDCl_3$) δ 8.10 (s, 1H, NH), 6.33 (s, 1H, α-pyrrole H), 4.26 (q, $J = 7.2$ Hz, 2H, CH_2CH_3), 2.47 (s, 3H, CH_3), 2.23 (s, 3H, CH_3), 1.33 (t, $J = 7.2$ Hz, 3H, CH_2CH_3); ^{13}C NMR (100 MHz, $CDCl_3$) δ 166.4, 135.9, 121.6, 114.2, 110.8, 59.1, 14.5, 14.1, 12.6; IR (KBr pellet) 3310, 2989−2925, 1665 cm^{-1}; HRMS (+ESI) *m*/*z* calcd for MH^+ 168.1025, found 168.1382.

8-[3,4-Bis(benzyloxy)phenyl]-2,6-bis(ethoxycarbonyl)-1,3,5,7-tetramethyl-4,4-diaza-*s*-indacene (7). To a flask charged with 100 mL of CH_2Cl_2 were added **3** (460 mg, 2.74 mmol), 3,4-bis(benzyloxy)benzaldehyde (438 mg, 1.38 mmol), and 3 drops of trifluoroacetic acid (TFA). The solution was stirred at 23 °C for 3 h, and 2,3-dichloro-5,6-dicyano-1,4-benzoquinone (DDQ; 343 mg, 1.51 mmol) was added in one portion. The mixture was stirred for 15 min and washed with an equal volume of brine. The organic fraction was dried with Na_2SO_4 and filtered and the crude mixture adsorbed onto 10 mL of basic alumina. The solvent was removed under vacuum, and the residue was purified by flash chromatography on basic alumina with a solvent gradient (4:1 → 1:1 hexanes/EtOAc). After removal of the solvent, the product was recrystallized

(8) Petrat, F.; Weisheit, D.; Lensen, M.; de Groot, H.; Sustmann, R.; Rauen, U. *Biochem. J.* **2002**, *363*, 137–147.
(9) Kikkeri, R.; Traboulsi, H.; Humbert, N.; Gumienna-Kontecka, E.; Arad-Yellin, R.; Melman, G.; Elhabiri, M.; Albrecht-Gary, A. M.; Shanzer, A. *Inorg. Chem.* **2007**, *46*, 2485–2497.
(10) Esposito, B. P.; Epsztejn, S.; Breuer, W.; Cabantchik, Z. I. *Anal. Biochem.* **2002**, *304*, 1–18.
(11) Xiang, Y.; Tong, A. J. *Org. Lett.* **2006**, *8*, 1549–1552.
(12) Xiang, Y.; Tong, A. J.; Jin, P. Y.; Ju, Y. *Org. Lett.* **2006**, *8*, 2863–2866.
(13) Jun, E. J.; Won, H. N.; Kim, J. S.; Lee, K. H.; Yoon, J. *Tetrahedron Lett.* **2006**, *47*, 4577–4580.
(14) Xu, Z. C.; Qian, X. H.; Cui, J. N. *Org. Lett.* **2005**, *7*, 3029–3032.
(15) Xu, Z. C.; Xiao, Y.; Qian, X. H.; Cui, J. N.; Cui, D. W. *Org. Lett.* **2005**, *7*, 889–892.
(16) Lim, N. C.; Pavlova, S. V.; Bruckner, C. *Inorg. Chem.* **2009**, *48*, 1173–1182.
(17) Gabe, Y.; Urano, Y.; Kikuchi, K.; Kojima, H.; Nagano, T. *J. Am. Chem. Soc.* **2004**, *126*, 3357–3367.
(18) Sunahara, H.; Urano, Y.; Kojima, H.; Nagano, T. *J. Am. Chem. Soc.* **2007**, *129*, 5597–5604.

from MeOH to afford the desired compound as yellow-brown needles (687 mg, 79.0%): TLC R_f = 0.70 (1:1 hexanes/EtOAc); mp 162−163 °C; ^{1}H NMR (400 MHz, $CDCl_3$) δ 7.49−7.29 (m, 10H, BnH), 7.02 (d, J = 8.0 Hz, 1H, ArH), 6.84 (d, J = 4.0 Hz, 1H, ArH), 6.78 (dd, J = 4.0, 8.0 Hz, 1H, ArH), 5.26 (s, 2H, BnH), 5.17 (s, 2H, BnH), 4.28 (q, J = 8.0 Hz, 4H, CH_2CH_3), 2.59 (s, 6H, CH_3), 1.58 (s, 6H, CH_3), 1.36 (t, J = 8.0 Hz, 6H, CH_2CH_3); ^{13}C NMR (100 MHz, $CDCl_3$) δ 165.3, 155.2, 149.7, 149.3, 146.3, 137.0, 136.7, 136.6, 130.0, 128.5, 128.0, 127.9, 127.5, 127.3, 122.5, 120.6, 115.9, 115.5, 71.3, 71.1, 59.7, 17.5, 14.4, 13.7; IR (KBr pellet) 3093, 3072, 3041, 2981−2920, 1695 cm^{-1}; HRMS (+ESI) m/z calcd for MH$^+$ 633.2965, found 633.2984.

8-[3,4-Bis(benzyloxy)phenyl]-2,6-bis(ethoxycarbonyl)-1,3,5,7-tetramethyl-4,4-difluoro-4-bora-3a,4a-diaza-*s*-indacene (9). To 100 mL of CH_2Cl_2 were added **7** (1.00 g, 1.59 mmol), triethylamine (Et_3N; 3.63 g, 35.9 mmol), and $BF_3\cdot OEt_2$ (5.60 g, 39.5 mmol). The solution was stirred at 23 °C for 1 h and washed with brine (2 × 150 mL). The organic fraction was dried with Na_2SO_4, filtered, and adsorbed onto 20 mL of silica gel. The solvent was removed under vacuum, and the mixture was purified by flash chromatography on silica (3:1 petroleum ether/EtOAc). The solvent was removed from the combined product fractions and recrystallized from MeOH to afford orange fibrous needles (932 mg, 86.3%): TLC R_f = 0.66 (1:1 hexanes/EtOAc); mp = 166−167 °C; ^{1}H NMR (400 MHz, $CDCl_3$) δ 7.46−7.27 (m, 10H, BnH), 7.03 (d, J = 8.4 Hz, 1H, ArH), 6.76 (d, J = 1.6 Hz, 1H, ArH), 6.71 (dd, J = 4.0, 8.0 Hz, 1H, ArH), 5.24 (s, 2H, BnH), 5.16 (s, 2H, BnH), 4.27 (q, J = 7.2 Hz, 4H, CH_2CH_3), 2.80 (s, 6H, CH_3), 1.57 (s, 6H, CH_3), 1.33 (t, J = 7.2 Hz, 6H, CH_2CH_3); ^{19}F NMR (376 MHz, $CDCl_3$) δ −142.9 (qd, J_{B-F} = 32 Hz, $^5J_{F-H}$ = 11 Hz); ^{13}C NMR (100 MHz, $CDCl_3$) δ 164.3, 159.4, 149.9, 149.7, 147.7, 145.5, 136.5, 136.3, 131.6, 128.6, 128.5, 128.1, 127.5, 127.3, 127.1, 122.4, 120.8, 115.9, 114.5, 71.3, 71.1, 60.2, 15.0, 14.3, 13.6; IR (KBr pellet) 3070−2889, 1709, 1684, 1522, 1313, 1189, 1109, 1010 cm^{-1}; HRMS (+ESI) m/z calcd for MH$^+$ 681.2947, found 681.3256.

8-(3,4-Dihydroxyphenyl)-2,6-bis(ethoxycarbonyl)-1,3,5,7-tetramethyl-4,4-difluoro-4-bora-3a,4a-diaza-*s*-indacene·0.2EtOAc (FerriBRIGHT). A mixture of **9** (210 mg, 420 μmol) and 10% Pd/C (31 mg, 10 mol %) in 6.0 mL of 1:1 EtOAc/MeOH was pressurized with 165 psi of H_2 in a sealed glass tube and irradiated at 25 W for 5 min at 70 °C. The mixture was filtered through a plug of Celite and the solvent removed under vacuum. The residue was recrystallized from MeOH/EtOAc (10:1) to afford the desired product as orange needles (101 mg, 65.9%). The persistence of EtOAc resonances of constant relative integration in the ^{1}H NMR spectrum after several washing/drying cycles with toluene indicates the existence of a stable solvate. Data for FerriBRIGHT: TLC R_f = 0.50 (1:1 EtOAc/petroleum ether); mp > 260 °C dec; ^{1}H NMR (400 MHz, DMSO-d_6) δ 9.49 (s, 1H, ArH), 9.36 (s, 1H, ArH), 6.91 (d, J = 8.0 Hz, 1H, ArH), 6.67 (d, J = 2.0 Hz, 1H, ArH), 6.59 (dd, J = 2.0, 8.0 Hz, ArH), 4.19 (q, J = 7.2 Hz, 4H, CH_2CH_3), 2.68 (s, 6H, CH_3), 1.72 (s, 6H, CH_3), 1.23 (t, J = 7.2 Hz, 6H, CH_2CH_3); ^{13}C NMR (100 MHz, $CDCl_3$) δ 163.8, 158.2, 147.5, 147.3, 147.2, 131.6, 124.3, 122.5, 119.1, 117.3, 115.3, 60.5, 15.0, 14.5, 13.9; IR (KBr pellet) 3429, 2993−2868, 1701, 1684, 1522, 1435, 1317, 1190, 1128, 1036 cm^{-1}; HRMS (+ESI) m/z calcd for MH$^+$ 501.2008, found 501.2232.

8-(*o*-Quinone)-2,6-bis(ethoxycarbonyl)-1,3,5,7-tetramethyl-4,4-difluoro-4-bora-3a,4a-diaza-*s*-indacene (FerriBRIGHT-Q). To a solution of FerriBRIGHT (100 mg, 200 μmol) in MeOH (5 mL) was added DDQ (100 mg, 440 μmol). The resulting heterogeneous mixture was stirred at 23 °C for 1 h and filtered and the filtrate evaporated to dryness. Flash chromatography on silica (9:1 CH_2Cl_2/MeOH) provided the product as a red-purple solid (21 mg, 21%): TLC R_f = 0.99 (9:1 CH_2Cl_2/MeOH); ^{1}H NMR (400 MHz, $CDCl_3$) δ 7.00 (dd, J = 2.0, 8.0 Hz, 2H, quinone), 6.74 (d, J = 8.0 Hz, 1H, quinone H), 6.57 (d, J = 2.0 Hz, quinone H), 4.35 (q, J = 8.0 Hz, 4H, CH_2CH_3), 2.86 (s, 6H, CH_3), 2.57 (s, 6H, CH_3), 1.39 (t, J = 8.0 Hz, 6H, CH_2CH_3); ^{13}C NMR (100 MHz, $CDCl_3$) δ 178.6, 178.0, 163.7, 161.7, 146.4, 145.9, 140.0, 138.0, 132.4, 130.7, 128.9, 123.5, 60.8, 60.7, 15.3, 15.1, 14.3; IR (KBr pellet) 3063, 2981−2875, 1697, 1668 cm^{-1}; HRMS (+ESI) m/z calcd for MH$^+$ 499.1852, found 499.1875.

8-[3,4-Bis(benzyloxy)phenyl]-1,3,5,7-tetramethyl-4,4-difluoro-4-bora-3a,4a-diaza-*s*-indacene·0.5EtOAc (8). A flask charged with 350 mL of CH_2Cl_2 was purged with N_2 for 15 min, and 3,4-bis(benzyloxy)benzaldehyde (**1**) (0.637 g, 2.00 mmol), 2,4-dimethylpyrrole (**2**) (0.381 g, 4.00 mmol), and 2 drops of trifluoroacetic acid were added. After the solution was stirred for 1 h at 23 °C, TLC analysis revealed complete conversion to the desired dipyrromethane (R_f = 0.78, silica, 1:1 EtOAc/hexanes). To the pale pink/red solution was added DDQ (0.499 g, 2.20 mmol) that was dissolved in a minimal amount of warm toluene. The addition of DDQ resulted in the immediate formation of a dark purple-red solution. After the solution was stirred at 23 °C for 1 h, TLC analysis revealed the presence of the desired dipyrrin (R_f = 0.75, basic alumina, 1:1 petroleum ether/EtOAc). To the mixture were added Hünig's base (4.0 mL, 23 mmol) and $BF_3\cdot OEt_2$ (3.0 mL, 24 mmol) sequentially via syringe. After the resulting solution was stirred for 5 min, TLC analysis revealed the presence of **8** (R_f = 0.65, silica, 1:1 EtOAc/hexanes). The solution was washed with 150 mL of brine, the organic phase was dried with Na_2SO_4, and the solids were removed by gravity filtration. The crude product was preadsorbed onto 10 mL of silica and dried under vacuum. Flash chromatography (4:1 hexanes/EtOAc) provided **8** as a bright orange powder (0.467 g, 43.5%) after solvent removal. The persistence of EtOAc resonances of constant relative integration in the ^{1}H NMR spectrum after several washing/drying cycles with toluene indicates the existence of a stable solvate. Data for **8**: mp 102−103 °C; ^{1}H NMR (400 MHz, $CDCl_3$) δ 7.50−7.30 (m, 10H, BnH), 7.04 (d, J = 8.0 Hz, 1H, ArH), 6.84 (d, J = 4.0 Hz, 1H, ArH), 6.77 (dd, J = 4.0, 8.0 Hz, 1H, ArH), 5.96 (s, 2H, BODIPY H), 5.26 (s, 2H, BnH), 5.20 (s, 2H, BnH), 2.56 (s, 6H, CH_3), 1.33 (s, 6H, CH_3); ^{13}C NMR (100 MHz, $CDCl_3$) δ 155.3, 149.3, 149.3, 143.2, 141.3, 136.7, 136.6, 131.6, 128.6, 128.5, 128.0, 127.9, 127.9, 127.5, 127.3, 121.0, 115.7, 114.8, 71.3, 71.0, 14.6, 14.2; IR (KBr pellet) 3122, 3091, 3066, 3033, 2960−2845, 1547, 1508, 1469 cm^{-1}; HRMS (+ESI) m/z calcd for M$^+$ 517.2463, found 517.2468.

8-(3,4-Dihydroxyphenyl)-1,3,5,7-tetramethyl-4,4-difluoro-4-bora-3a,4a-diaza-*s*-indacene (10). A mixture of 10% Pd/C (500 mg, 56 mol % Pd) and **8** (400 mg, 746 μmol) in 10 mL of 1:1 MeOH/CH_2Cl_2 was stirred under a H_2 atmosphere (1 atm) at 23 °C for 20 h. The mixture was filtered through Celite, and the filter cake was washed with small portions of MeOH and EtOAc. Removal of solvent under vacuum afforded the product as a red powder (298 mg, 99.9%). The product was preadsobed onto 5 mL of silica and loaded onto a silica column. Flash chromatography (3:2 petroleum ether/EtOAc) was used to provide highly pure material for spectroscopy (149 mg, 49.7%): TLC R_f = 0.40 (1:1 EtOAc/hexanes), mp > 260 °C dec; ^{1}H NMR (400 MHz, DMSO-d_6) δ 9.25 (s, 2H, ArH), 9.36 (s, 1H, ArH), 6.86 (d, J = 8.0 Hz, 1H, ArH), 6.61 (d, J = 2.0 Hz, 1H, ArH), 6.52 (dd, J = 2.0, 8.0 Hz, 1 H), 2.40 (s, 6H, CH_3), 1.46 (s, 6H, CH_3); ^{13}C NMR (100 MHz, $CDCl_3$) δ 154.8, 146.7, 146.6, 143.2, 131.5, 125.0, 121.5, 119.0, 116.9, 115.3, 14.6, 14.5; IR (KBr pellet) 3504, 3446, 2968−2870, 1543, 1508 cm^{-1}; HRMS (+ESI) m/z calcd for MH$^+$ 357.1506, found 357.1608.

8-(*o*-Quinone)-1,3,5,7-tetramethyl-4,4-difluoro-4-bora-3a,4a-diaza-*s*-indacene (11). A solution of **10** (40 mg, 122 μmol) was mixed with a solution of $FeCl_3$ (911 mg, 5.61 mmol) in 10 mL of MeOH and the resulting mixture stirred at 23 °C for 10 min. The mixture was diluted with H_2O (40 mL) and extracted with $CHCl_3$ (3 × 20 mL), and the organic fractions were pooled and evaporated to dryness. Flash chromatography on silica (7:3 petroleum ether/EtOAc) provided the product as a red-purple powder (18 mg, 45%): TLC R_f = 0.30 (silica, 7:3 petroleum ether/EtOAc); ^{1}H NMR (400 MHz, $CDCl_3$) δ 7.00 (dd, J = 2.0, 8.0 Hz, 2H, quinone), 6.65 (d, J = 8.0 Hz, 1H, quinone H), 6.55 (d, J = 2.0 Hz, quinone H), 6.12

(s, 2H, BODIPY H), 2.58 (s, 6H, CH_3), 2.22 (s, 6H, CH_3); ^{13}C NMR (100 MHz, $CDCl_3$) δ 178.9, 178.4, 158.0, 146.9, 141.6, 140.9, 134.3, 131.8, 130.5, 128.5, 122.3, 15.7, 14.8; IR (KBr pellet) 3098, 3081, 2963−2855, 1694, 1667 cm^{-1}; HRMS (+ESI) *m*/*z* calcd for MH^+ 357.1586, found 357.1590.

General Spectroscopic Methods. All solutions were prepared with spectrophotometric grade solvents. Absorption spectra were recorded on a Cary 50 UV−vis spectrophotometer under the control of a Pentium IV-based PC running the manufacturer-supplied software package. Spectra were routinely acquired at 25 °C in 1 cm path length quartz cuvettes with a total volume of 3.0 mL. Fluorescence spectra were recorded on a Hitachi F-4500 spectrophotometer under the control of a Pentium-IV PC running the FL Solutions 2.0 software package. Excitation was provided by a 150 W Xe lamp (Ushio Inc.) operating at a current of 5 A. Spectra were routinely acquired at 25 °C in a 1 cm quartz cuvette with a total volume of 3.0 mL using, unless otherwise stated, 5 nm slit widths and a photomultiplier tube power of 700 V.

UV−Vis Experiments with Ferrozine and Neocuproine. Commercially available ferrozine and neocuproine indicators were dissolved in MeOH to make 10 mM stock solutions. Stock solutions of anhydrous $FeCl_3$ and $CuCl_2$ (10 mM) were prepared in MeOH and passed through a 2 μm cellulose filter prior to use. Solutions were prepared with a 10-fold excess of indicator and $FeCl_3$ or $CuCl_2$ and allowed to equilibrate for 0.5 h prior to the spectra being recorded.

Quantum Yield. Quantum yields were calculated by measuring the integrated emission area of the corrected spectra and comparing that value to the area measured for fluorescein in 0.1 N NaOH when excited at 490 nm ($\Phi_{fl} = 0.85$).[19] The quantum yields for FerriBRIGHT, FerriBRIGHT-Q, and compounds **10** and **11** were then calculated using eq 1, where *F* represents the area under the emission spectra for the standard and samples, η is the refractive index of the solvent, and Abs is the absorbance at the excitation wavelength selected for the standard and samples. Emission was integrated between 502 and 700 nm ($\lambda_{ex} = 490$ nm,10^{-6} M, $Abs_{490} \approx 0.1$).

$$\Phi_{fl}^{sample} = \Phi_{fl}^{standard}\left(\frac{F^{sample}}{F^{standard}}\right)\left(\frac{\eta^{sample}}{\eta^{standard}}\right)\left(\frac{Abs^{standard}}{Abs^{sample}}\right) \quad (1)$$

Titration of FerriBRIGHT with $Ga(NO_3)_3$, $[Co(NH_3)_5Cl]Cl_2$, and $FeCl_3$. To investigate the metal-induced oxidation of FerriBRIGHT, a stock solution of $FeCl_3$ dissolved in MeOH (7.6 mM) was added in 40 μL aliquots to a 10 μM solution of FerriBRIGHT, and emission spectra were recorded every minute for 1 h. The excitation wavelength was $\lambda_{ex} = 498$ nm, the excitation slit widths were set at 10 nm, and the emission slit widths were set at 5.0 nm. The area under the emission spectra was integrated over a wavelength range of 505−600 nm. The experiment was repeated with a stock solution of $[Co(NH_3)_3Cl]Cl_2$ (1.7 mM). A stock of $Ga(NO_3)_3$ (7.8 mM) in 1:2 DMSO/MeOH was added to a magnetically stirred solution of FerriBRIGHT (1.5 μM) in 1−25 μL increments. Absorbance and emission spectra were recorded sequentially until no further changes were observed. To assess the binding stoichiometry and conditional binding constant (K_f') of FerriBRIGHT with Ga(III), the method of continuous variation was performed in triplicate. To acquire absorbance spectra for solutions containing between 0.0 and 9.0 μM Ga(III), the method of reciprocal dilutions was used. The spectrum of a 3000 μL methanolic solution of 10 μM FerriBRIGHT was recorded. To prepare a solution containing 1 μM Ga(III) and 9 μM FerriBRIGHT in the first iteration ($n = 1$), 300 μL of the FerriBRIGHT solution was removed from the cuvette and replaced with 300 μL of stock 10 μM methanolic $Ga(NO_3)_3$, and the absorbance spectrum was recorded. The process was repeated for $n = 2-9$ iterations by removing from the cuvette and replacing with $1/(11 - n) \times 3000$ μL of stock Ga(III). Difference spectra for $n = 1-9$ were calculated from $Abs_n - Abs_{Lig}\chi_{Lig}$, where Abs_n is the absorbance spectrum for the *n*th iteration, Abs_{Lig} is the absorbance spectrum of FerriBRIGHT alone, and χ_{Lig} is the mole fraction of FerriBRIGHT. The resulting difference in absorbance was plotted as a function of the wavelength. Job's plots were prepared using absorbance data at 485 and 498 nm. All spectroscopic measurements were performed in triplicate.

Fluorescence Selectivity of FerriBRIGHT with Various Metal Cations and Oxidants. Commercially available metal chloride salts were used in these experiments. All the salts were prepared as stock methanol solutions. A 50-fold excess of each of the metals was added to 10 μM solutions of FerriBRIGHT in MeOH. Fluorescence spectra were recorded after 0.5 h. The spectra were registered again to ensure no further changes had taken place. Stock solutions of $K_3Fe(CN)_6$, DDQ, *t*-BuO_2H, and ceric ammonium nitrate (CAN) were also prepared in methanol. Stock solutions of H_2O_2, KO_2, and NaOCl were prepared in 0.17 M Na_2HPO_4. A 1:1 mixture of NaOCl (100 μM) and H_2O_2 (100 μM) was prepared in the presence of 10 μM FerriBRIGHT to generate $^1O_2$ in situ. A 1:1 mixture of $FeSO_4$ and ethylenediaminetetraacetic acid (EDTA; 100 μM) was prepared in the presence of 10 μM FerriBRIGHT and H_2O_2 (100 μM) to generate $HO^\bullet$ in situ. A stock solution of L-ascorbic acid (0.16 M) was prepared in H_2O, and a 9.2 μL aliquot was added to an equilibrated methanolic solution of FerriBRIGHT (10 μM) and CAN (500 μM).

Computational Methods. Orbital energies were calculated using Gaussian 03 at the B3LYP/6-31G level of theory. To reduce the calculation time, the catechol fragment was modeled independent of the BODIPY fragment. The driving force of the eT was calculated using the Rehm−Weller equation (eq 2).[20] The literature value for the one-electron oxidation of catechol ($E(D^+/D)$)[21] and the charge separation term (C)[22] were used in the calculations. The calculation of the relative free energy ($\Delta\Delta G_{PeT}$) demonstrates that the presence of the electron-withdrawing ethyl esters at the 2,6-positions of the BODIPY fluorophore favors PeT by 0.34 eV (~30 kJ/mol).

$$\Delta G_{PeT} = E_{1/2}\left(\frac{D^+}{D}\right) - E_{1/2}\left(\frac{A}{A^-}\right)\Delta E_{00} - C \quad (2)$$

$\Delta G_{PeT}^{X=CO_2Et} = 0.1$ eV $-$ (−0.85 eV) $-$ 2.48 eV $-$ 0.72 eV $= -2.25$ eV
$\Delta G_{PeT}^{X=H} = 0.1$ eV $-$ (−1.19 eV) $-$ 2.48 eV $-$ 0.72 eV $= -1.91$ eV
$\Delta\Delta G_{PeT} = -2.25$ eV $-$ (−1.91 eV) $= -0.34$ eV

Results and Discusion

Design Rationale. BODIPY (4,4-difluoro-4-borata-3a-azonia-4a-aza-*s*-indacene) fluorophores are useful components of fluorescent sensors because they possess large absorbance bands with large molar absorptivities in the visible region of the electromagnetic spectrum ($\varepsilon \approx 40000-110000$ cm^{-1} M^{-1}).[23] The fluorescence quantum yields of these fluorophores approach unity with typical values varying between 60% and 90%. In addition to spectroscopic properties, the emission intensity of BODIPY fluorophores can be tuned systematically by modulating the PeT from pendant aryl rings in a manner similar to that of investigations with fluorescein derivatives.[22,24,25] Systems that

(19) Parker, C. A.; Rees, W. T. *Analyst* **1960**, *85*, 587–600.
(20) Rehm, D.; Weller, A. *Isr. J. Chem.* **1970**, *8*, 259–71.
(21) Eberson, L. *Adv. Free Radical Biol. Med.* **1985**, *1*, 19–90.
(22) Miura, T.; Urano, Y.; Tanaka, K.; Nagano, T.; Ohkubo, K.; Fukuzumi, S. *J. Am. Chem. Soc.* **2003**, *125*, 8666–8671.
(23) Ulrich, G.; Ziessel, R.; Harriman, A. *Angew. Chem., Int. Ed.* **2008**, *47*, 1184–1201.
(24) Weibel, N.; Charbonniere, L. J.; Guardigli, M.; Roda, A.; Ziessel, R. *J. Am. Chem. Soc.* **2004**, *126*, 4888–4896.

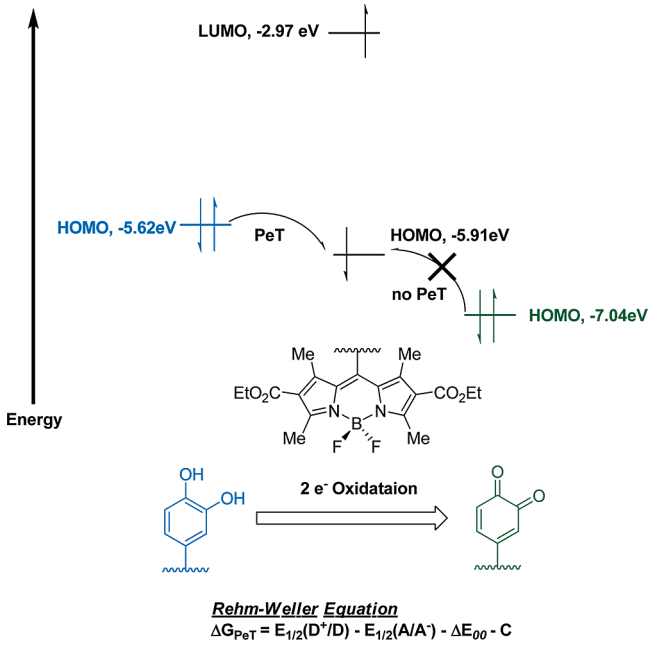

Figure 1. Frontier orbital diagram of FerriBRIGHT. In the reduced form the catechol participates in PeT with the excited state of the fluorophore. Upon 2e$^-$ oxidation the HOMO of the quinone lies below the S_1 excited state, preventing PeT. The HOMO energy of the BODIPY fragment where the ethyl esters are replaced with H atoms, **10**, is −5.42 eV (Scheme 1). This orbital is higher in energy than the HOMO of catechol, so no PeT quenching of emission is predicted. Orbital energies were calculated using Gaussian 03 at the B3LYP/6-31G level of theory. The driving force of eT can also be calculated using the Rehm−Weller equation, where $E(D^+/D)$ is the oxidation potential of catechol, $E(A/A^-)$ is the reduction potential of the acceptor, ΔE_{00} is the excitation energy of the acceptor, and C is the charge separation term.

are conjugatively uncoupled can possess a nonradiative PeT deactivation channel as long as the donor's HOMO is energetically interstitial to the HOMO−LUMO gap of the fluorophore (Figure 1). The thermodynamic driving force behind PeT was assessed using the Rehm−Weller equation.[20] The reported $E(A/A^-)$ for the BODIPY dye used in this study is −0.87 eV (MeCN/SCE), which is +0.32 eV more positive than the value reported for the analogous fluorophore that possesses H atoms at the 2,6-positions.[18] This makes the BODIPY chromophore more susceptible to reduction, facilitating PeT. By calculating the HOMO energy for catechol ($HOMO_{catechol} = -5.62$ eV using the B3LYP/6-31G level of theory with Gaussian 03[26] and comparing that result to the values for known compounds, we predicted that FerriBRIGHT would be engaged in PeT, resulting in quenched fluorescence emission. The name FerriBRIGHT is derived from the compound's ability to image ferric iron with a bright fluorescence signal.

Synthesis. The desired catechol−BODIPY dyad FerriBRIGHT was synthesized from the dibenzyl-protected catechol **1** and the trisubstituted pyrrole **3**, which were prepared in 94% and 78% yields, respectively, using literature procedures (Scheme 1).[27,28] The precursor to compound **3**, tetrasubstituted pyrrole **3a**, was constructed using the Knorr pyrrole synthesis. The use of concentrated HCl to remove the *tert*-butoxy ester of **3a** gave a clean product slate with a >30% enhancement of the isolated yield than with the use of catalytic pTsOH, as originally reported.[29] Moreover, compound **3** did not require chromatography for purification if HCl was used during the acid-mediated hydrolysis/decarboxylation step.

Dyes **8** and **9** were constructed using a typical one-pot, three-step procedure that has been utilized in the construction of numerous 8-substituted BODIPY fluorophores.[23] When applied to compound **9**, the one-pot procedure gave a poor overall yield of the desired material after column chromatography on silica gel (∼10%). This is consistent with literature reports when ester or acyl groups are present at the 2,6-positions of the chromophore.[17] When replaced with hydrogen atoms as in compound **8** (X = H), the one-pot procedure afforded the BODIPY dye in 44% yield, a marked improvement as compared to the yield of compound **9**. Optimization of this procedure was sought to prepare gram quantities of **9**. TLC analysis of each step in the preparation of dye **9** revealed clean formation of both the dipyrromethane **5** after 2−3 h and dipyrrin **7** after 15 min; however, introduction of $BF_3\cdot OEt_2$ in the third step of the procedure led to the formation of several byproducts. To avoid these byproducts, dipyrrin **7** was isolated from the reaction mixture via column chromatography on basic alumina and recrystallized from MeOH in 79% yield. The purified dipyrrin was reacted with excess $BF_3\cdot OEt_2$ in fresh CH_2Cl_2, resulting in the clean formation of BODIPY dye **9**, as evidenced by TLC analysis after 1 h. The desired material was obtained in 86% yield after chromatography on silica gel and recrystallization from MeOH, which resulted in an improved 68% overall yield of BODIPY **9**.

The last step in the reaction sequence of FerriBRIGHT requires removal of the benzyl protecting groups on the catechol moiety. Upon exposing **8** to standard hydrogenolysis conditions with ∼1 atm of gaseous H_2 and catalytic Pd/C, compound **10** was prepared and isolated in 50% yield after column chromatography. When the same conditions were applied to compound **9**, however, TLC analysis showed an incomplete conversion to FerriBRIGHT after 18 h and the concomitant development of a highly colored byproduct. Microwave irradiation can accelerate the rate of and improve the yields of challenging reactions, notably metal-catalyzed hydrogenations.[30] Typically, these microwave-assisted hydrogenations are carried out using transfer hydrogenation conditions with excess ammonium formate to generate H_2 in situ; however, a simple and efficient procedure that utilizes gaseous H_2 at moderate pressures and temperature was recently reported.[30] Using the apparatus described by Leadbeater,[31] **9** was hydrogenated at 165 psi of gaseous H_2 at 70 °C. TLC analysis after 5 min of irradiation showed complete consumption of the starting material with formation of FerriBRIGHT and a small amount of a byproduct, which was easily removed after recrystallization to afford the desired material in 66% yield as orange needles. The development of this microwave-assisted double deprotection reaction will greatly assist future synthetic efforts.

Fluorescence Properties. The absorbance spectra of FerriBRIGHT in several organic solvents displayed sharp $S_1 \leftarrow S_0$ transitions with a $\lambda_{max} \approx 500$ nm and molar absorptivities that varied between 64800 and 115700 $cm^{-1}M^{-1}$ (Figure 2). Spectra

(25) Mineno, T.; Ueno, T.; Urano, Y.; Kojima, H.; Nagano, T. *Org. Lett.* **2006**, *8*, 5963–5966.
(26) Frisch, M. J.; et al. *Gaussian 03*, revision C.02; Gaussian, Inc.: Wallingford, CT, 2004.
(27) Li, C. C.; Xie, Z. X.; Zhang, Y. D.; Chen, J. H.; Yang, Z. *J. Org. Chem.* **2003**, *68*, 8500–8504.
(28) Sun, L.; et al. *J. Med. Chem.* **2003**, *46*, 1116–1119.
(29) Treibs, A.; Hintermeier, K. *Chem. Ber.* **1954**, *87*, 1167–74.
(30) Vanier, G. S. *Synlett* **2007**, 131–135.
(31) Kormos, C. M.; Leadbeater, N. E. *Synlett* **2007**, 2006–2010.

Scheme 1. Synthesis of FerriBRIGHT

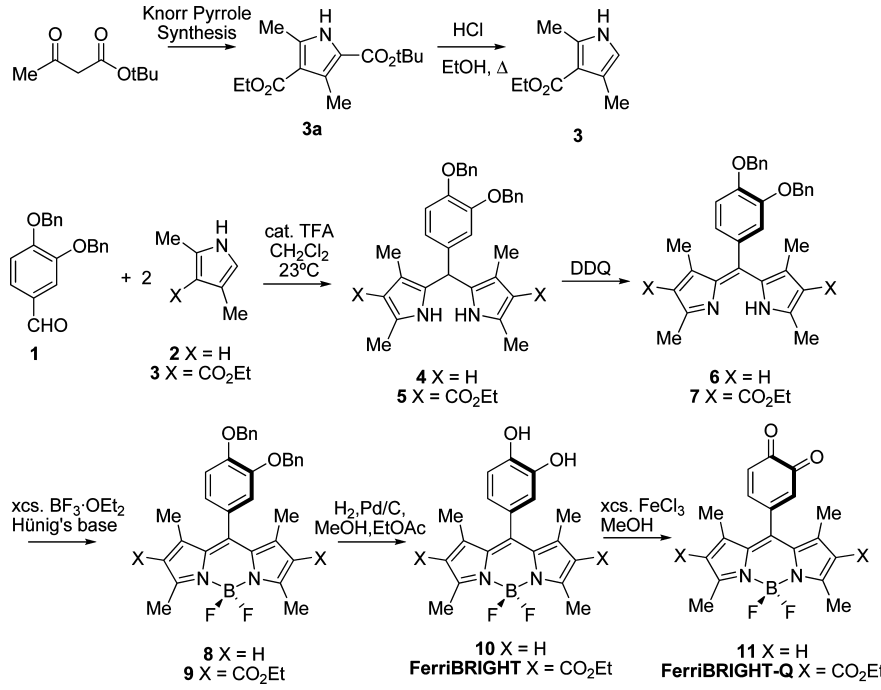

of FerriBRIGHT could not be obtained in pure H_2O because of limited solubility; however, homogeneous solutions with sharp spectral features could be obtained in aqueous media that contained 5% by volume Trition X-100, a nonionic detergent comprised of poly(ethylene glycol) derivatives. The measured fluorescence of FerriBRIGHT was quite dim, but a polarity dependence was observed in the quantum yield of fluorescence (Φ_{fl}) when measured in various solvents (Table 1). In polar media, such as MeOH, the quantum yield was quite small ($\Phi_{fl} \approx 0$); however, in less polar solvents, such as CH_2Cl_2 or $C_6H_5CH_3$, the fluorescence quantum yield increased to 0.056 or 0.256, respectively (Table 1). The Φ_{fl} solvent dependency is likely related to the PeT between the pendant catechol ring and the BODIPY fluorophore. Electron transfer for similar BODIPY- and fluorescein-derived dyads occurs readily in polar solvents,

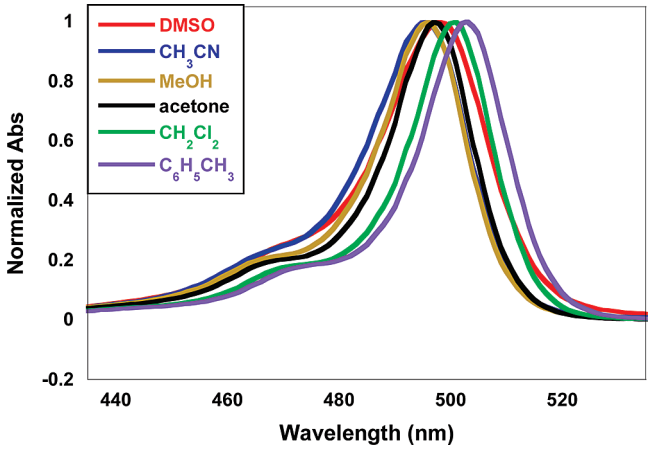

Figure 2. Absorbance spectra of 10 μM FerriBRIGHT in various solvents. Each spectrum was normalized to unity by dividing the measured absorbance by the absorbance at λ_{max}.

Table 1. Quantum Yields of Fluorescence of **10** and FerriBRIGHT in Various Solvents

solvent	Φ_{fl}(**10**)	Φ_{fl}(FerriBRIGHT)
$C_6H_5CH_3$	0.593	0.256
CH_2Cl_2	0.326	0.056
acetone	0.036	0.002
MeOH	0.007	~0[a]
MeCN	0.035	~0[a]
DMSO	0.002	~0[a]

[a] Quantum yields were determined using fluorescein in 0.1 M NaOH as a standard (λ_{ex} = 490 nm, Φ_{fl} = 0.85) at 25 °C.[19] The concentrations were adjusted to 1−2 μM, where the absorbance was ~0.1 at 490 nm. The emission spectra were obtained at λ_{ex} = 490 nm (integrated emission intensity from 502 to 700 nm). The excitation slit width was 2.5 nm, and the emission slit width was 5.0 nm. The calculated quantum yield of fluorescence was <0.001 and could not be determined accurately.

quenching fluorescence.[32] In nonpolar solvents, the oxidation potential of the pendant ring became more positive whereas the reduction potential of the BODIPY became more negative, which results in a larger free energy change of PeT (ΔG_{PeT}). Consequently, in nonpolar media, the PeT between the pendant ring and BODIPY fluorophore is extinguished and the fluorescence of the dyad is restored.

Exposing FerriBRIGHT to excess $FeCl_3$ in aerobic MeOH led to a 29-fold increase in the fluorescence emission intensity (Figure 3). The increase in the observed emission intensity was attributed to Fe(III)-mediated oxidation of the catechol ring to the corresponding *o*-quinone.[33] The intermediate semiquinone is short-lived with unsubstituted catechols and oxidizes rapidly to the quinone in the presence of excess metal at room temperature.[34] Likewise, the *o*-quinones FerriBRIGHT-Q and **11** were independently synthesized from either excess $FeCl_3$ or

(32) Koide, Y.; Urano, Y.; Kenmoku, S.; Kojima, H.; Nagano, T. *J. Am. Chem. Soc.* **2007**, *129*, 10324–10325.
(33) Avdeef, A.; Sofen, S. R.; Bregante, T. L.; Raymond, K. N. *J. Am. Chem. Soc.* **1978**, *100*, 5362–70.
(34) Kamau, P.; Jordan, R. B. *Inorg. Chem.* **2002**, *41*, 3076–3083.

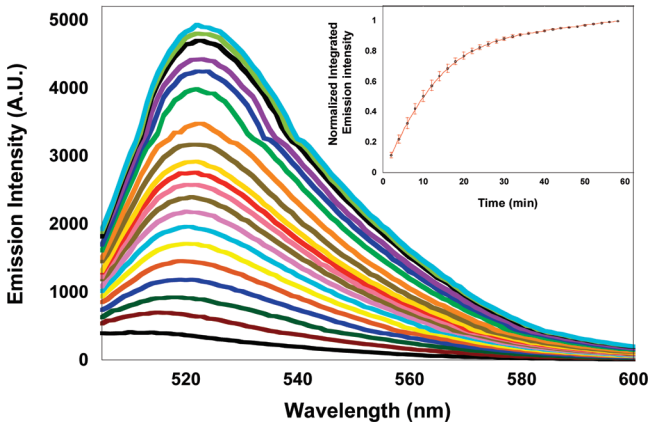

Figure 3. Oxidation of 10 μM FerriBRIGHT with 10 equiv of $FeCl_3$ in MeOH. The emission spectra were automatically recorded every minute for 1 h. Excitation was provided at 498 nm with an excitation slit width of 5.0 nm and an emission slit width of 10 nm. Inset: changes in integrated fluorescence emission between 505 and 600 nm over 1 h with error bars corresponding to variations over three trials.

Table 2. Spectroscopic Properties of **10**, **11**, FerriBRIGHT, and FerriBRIGHT-Q in MeOH

compound	$\lambda_{ex\text{-}max}$/nm (ε/cm^{-1}M^{-1})	$\lambda_{em\text{-}max}$/nm	Φ_{fl}
FerriBRIGHT	496(119000)	510	$\sim 0^a$
FerriBRIGHT-Q	501 (53400)	516	0.027
10	498 (93300)	508	0.007
11	502 (50200)	509	0.007

[a] Quantum yields were determined using fluorescein in 0.1 M NaOH as a standard (λ_{ex} = 490 nm, Φ_{fl} = 0.85) at 25 °C.[19] The concentrations were adjusted to 1−2 μM, where the absorbance was ~0.1 at 490 nm. The emission spectra were obtained at λ_{ex} = 490 nm (integrated emission intensity from 502 to 700 nm). The excitation slit width was 2.5 nm, and the emission slit width was 5.0 nm. The calculated quantum yield of fluorescence was <0.001 and could not be determined accurately.

DDQ in aerobic MeOH, purified, and characterized (vide infra), which allowed for a reliable inspection of the spectral changes that occur upon oxidation (Figure 3). Unexpectedly, the FerriBRIGHT-Q did not require trapping of the quinone with agents such as benzenesulfinic acid to permit characterization. FerriBRIGHT-Q and **11** survived chromatographic separation and could be stored for indefinite amounts of time at room temperature. In MeOH, the $S_1 \leftarrow S_0$ transition of the BODIPY chromophore of FerriBRIGHT occurs at 496 nm ($\varepsilon \approx 119000$ cm^{-1} M^{-1}), which undergoes a small bathochromic shift of ~5 nm to 501 nm ($\varepsilon \approx 53400$ cm^{-1} M^{-1}) upon oxidation. The corresponding emission spectra were recorded in MeOH when excited with 490 nm light. FerriBRIGHT possesses a small fluorescence with maximal emission at 510 nm, whereas FerriBRIGHT-Q is more emissive with a maximal emission that has been bathochromically shifted by 6 nm to 516 nm. The measured quantum yields of compounds **10** and **11** are identical ($\Phi_{fl} \approx 0.007$), while the measured quantum yield of FerriBRIGHT-Q (Φ_{fl} = 0.026) is notably larger than that of FerriBRIGHT ($\Phi_{fl} \approx 0$) (Table 2). Oxidation to the *o*-quinone removes 2 electrons from the donor, and the HOMO of the PeT quencher is lowered by 1.17 eV as calculated by Gaussian ($HOMO_{quinine}$ = −6.79 eV). This result suggests that upon oxidation the HOMO of the BODIPY-pendant ring is no longer energetically able to mediate fluorescence quenching, allowing for detection of redox changes (Figure 1). The results from the quantum mechanical calculations also rationalize the inability of **10** to respond to the catechol to quinone oxidation. The

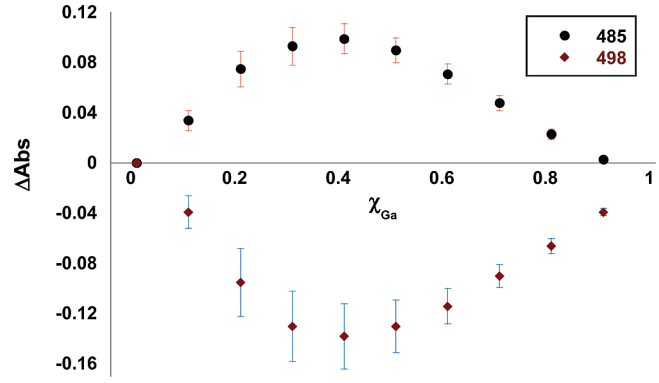

Figure 4. Job's plot for FerriBRIGHT with Ga(III). The maximal ABS difference occurred at $\chi_{Ga} = 0.34 \pm 0.01$ when measured at 485 and 498 nm. Tangents to the curve at χ_{Ga} = 0.1−0.3 and χ_{Ga} = 0.5−0.7 were calculated using a linear least-squares fit of the data. Error bars represent variation over two independent measurements.

SOMO of the S_1 state of the BODIPY acceptor in **10** lies 0.42 eV higher in energy ($SOMO_{BODIPY}$ = −5.42 eV) than in FerriBRIGHT. The lack of matching between the donor and acceptor energies prevents PeT quenching in the initial molecule, which short-circuits the fluorescence switch.

Introduction of fewer than 10 equiv of Fe(III) to FerriBRIGHT led to a more sluggish increase in the emission intensity; however, the oxidation of substrate would not allow an accurate analysis of binding constants. To assess the conditional binding of FerriBRIGHT and Fe(III), binding studies were performed with a redox-inactive analogue of ferric iron, Ga(III). The method of continuous variation was used to assess the binding of $Ga(NO_3)_3$ and FerriBRIGHT in methanolic solution. Analysis of Job's plot reveals that the dominating species under these conditions is a 1:2 Ga(III)/FerriBRIGHT complex, where maximal changes in the UV−vis spectra occurred at $\chi_{Ga} \approx 0.33$ (Figure 4). The conditional binding constant log β_{12}' was estimated at 13.3 ± 0.2 using conventional analysis.[35] The steric bulk of the ligand likely hinders the formation of a coordinatively saturated 1:3 Ga(III)/FerriBRIGHT complex. Emission spectra were also recorded after addition of Ga(III) titrant to a 1.5 μM solution of FerriBRIGHT in MeOH. The measured emission intensity continually increased over the course of the titration, which demonstrates the possibility of metal ion sensing. A maximum 2.8-fold increase in the integrated emission intensity was observed when ≥100 equiv of Ga(III) had been added (Figure 5). Presumably the catechol ring is stabilized upon metal ion coordination, partially attenuating the quenching PeT process.[36] Presumably there is self-quenching by the two proximal BODIPY fluorophores in the 1:2 complex because maximum emission intensity is achieved when high Ga(III) concentrations bias the formation of a 1:1 complex. The integrated emission at Ga(III) concentrations between 30 and 90 μM shows an apparent equivalence point, and analysis of the fluorescence response above this point is consistent with a 1:1 complex with a log K_{11}' of ~5 (Figure 5, inset). Work is currently under way to introduce a redox-inactive group on the BODIPY dye with the aim of rationally designing turn-on fluorescent sensors for Fe(III).

To confirm the switching mechanism experimentally, fluorescence measurements were taken upon exposure of Ferri-

(35) Likussar, W.; Boltz, D. F. *Anal. Chem.* **1971**, *43*, 1265–72.
(36) Callan, J. F.; de Silva, A. P.; Magri, D. C. *Tetrahedron* **2005**, *61*, 8551–8588.

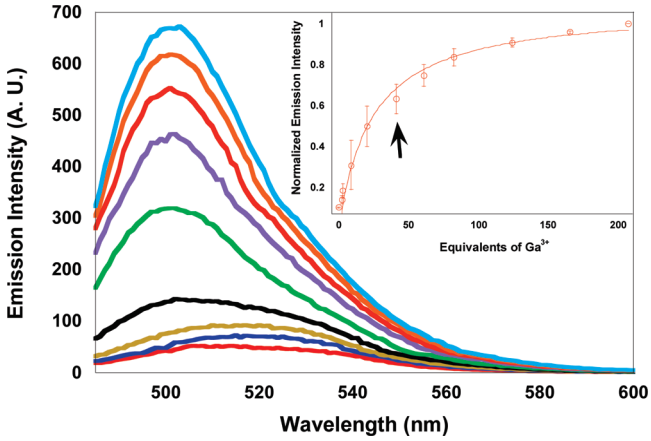

Figure 5. Saturation of 1.5 μM FerriBRIGHT in MeOH with $Ga(NO_3)_3$. Spectra were taken at 0, 2, 3, 9, 20, 41, 61, 82, 120, 160, and 210 equiv of Ga^{3+}. Each spectrum was corrected for dilution by multiplying the measured absorption and integrated emission intensity by the inverse of the dilution factor. The emission intensity was integrated from 502 to 600 nm. Error bars represent variation over three trials. Excitation was provided at 490 nm with an excitation slit width of 10.0 nm and an emission slit width of 5 nm. Inset: changes in integrated fluorescence emission between 502 and 600 nm with increasing equivalents of Ga^{3+}. Error bars correspond to the variation among three trials. The observation of a reproducible equivalence point between 30 and 90 μM Ga^{3+} (20−60 equiv) is attributed to the conversion of a 2:1 L/M complex into a 1:1 species.

BRIGHT to a host of oxidants, ROS, and metal cations (Figure 6). Large fluorescence enhancements were observed with aerobic methanolic solutions of Cu(II), CAN, and DDQ, all which affect the desired oxidation.[34,37,38] Adding excess sodium ascorbate to an equilibrated solution of FerriBRIGHT and CAN partially reduced the quinone back to the catechol, resulting in the reduction of the measured emission intensity. In the case of Fe(III) and Cu(II) the concomitant formation of 2 equiv of Fe(II) and Cu(I) was measured directly using commercially available spectroscopic probes (Figure 7). When FerriBRIGHT was oxidized with Fe(III) in the presence of ferrozine, the solution turned red with an MLCT band that developed at 560 nm indicating the formation of the $[Fe(ferrozine)_3]^{4-}$ complex.[39] Likewise, the Cu(I) indicator neocuproine was used to spectroscopically measure the reduced form of the metal. Development of an MLCT band at 460 nm of the resulting orange/yellow-colored solution is consistent with the formation of the $[Cu(neocuproine)_2]^{+}$ complex.[40] The complexes were not observed when FerriBRIGHT was absent from solutions of the metal and indicator.

In the presence of 10 equiv of Co(III), changes in the emission intensity were observed over a period of 24 h (Figure 8). The slow rate of oxidation is explained by the substitutionally inert nature of the low-spin d^6 Co(III) cation, which undergoes sluggish ligand exchange reactions.[41] These data suggest that coordination between FerriBRIGHT and Co(III) must occur prior to oxidation. Coordination of the catechol moiety to a binding partner, followed by either inner-sphere or outer-sphere electron transfer, may ultimately play a role in the selectivity of the fluorescence response of FerriBRIGHT to various species.

(37) Uchimiya, M.; Stone, A. T. *Geochim. Cosmochim. Acta* **2006**, *70*, 1388–1401.
(38) Fischer, A.; Henderson, G. N. *Synthesis* **1985**, 641–3.
(39) Stookey, L. L. *Anal. Chem.* **1970**, *42*, 779–81.
(40) Besada, A. *Anal. Lett.* **1988**, *21*, 1917–25.
(41) Diebler, H.; Eigen, M.; Ilgenfritz, G.; Maass, G.; Winkler, R. *Pure Appl. Chem.* **1969**, *20*, 93–115.

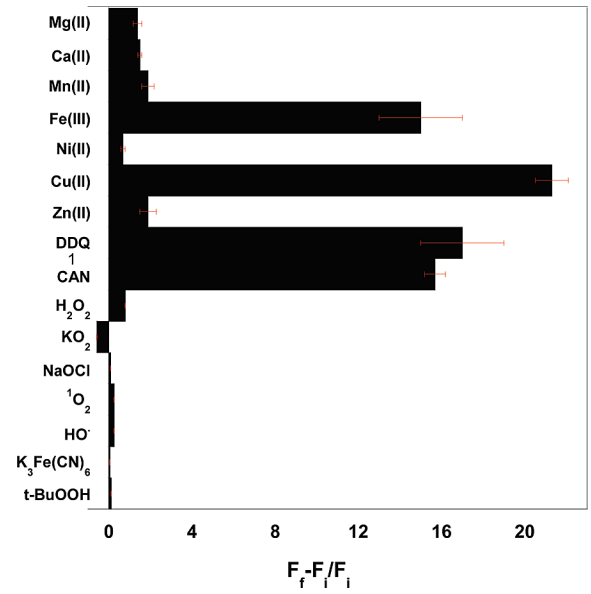

Figure 6. Fluorescence response of 10 μM FerriBRIGHT to various oxidizing species. Bars represent the difference between the integrated final fluorescence response (F_f) and the integrated initial fluorescence response (F_i) divided by F_i. Emission was integrated between 480 and 700 nm. All measurements were made after the addition of 50 equiv of metal cations, DDQ, CAN, or ROS to FerriBRIGHT in MeOH at 25 °C. A mixture of NaOCl and H_2O_2 was used to generate $^1O_2$. A mixture of $[Fe(EDTA)]^{2-}$ and H_2O_2 was used to generate HO•. Excitation was provided at 465 nm, with excitation and emission slit widths of 10 and 5 nm, respectively. Error bars correspond to variations over three trials. For the species where no significant emission change was observed, the error bars are too small to be visible.

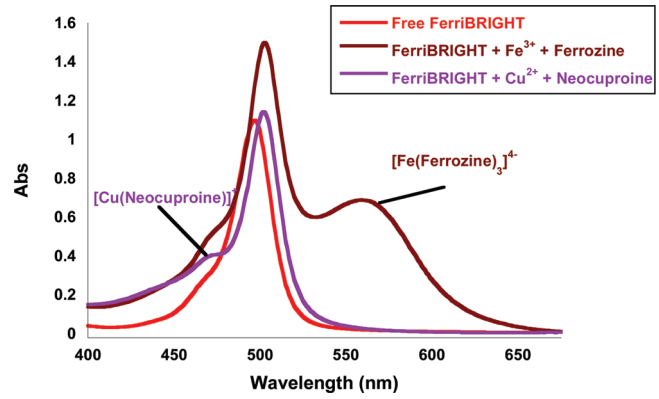

Figure 7. Absorbance spectra of 10 μM FerriBRIGHT (MeOH) in the presence of 10 equiv of Fe(III) or Cu(II) and with 10 equiv of ferrozine or neocuproine.

Preliminary experiments suggest that the rate of metal-mediated oxidation depends not only on the coordination but also on the concentrations of O_2, M^{n+}, and FerriBRIGHT. Accurate determination of oxidative stress levels using probes that utilize a catechol → quinone transformation will require a detailed kinetic analysis that also accounts for the reoxidation of reduced metal as well as a consideration of the redox potential of the cellular environment in which the probes are deployed.

The emission intensity of FerriBRIGHT did not change significantly when exposed to excess Zn(II), Mg(II), and Ca(II), all of which are redox inactive but are ubiquitous metal cations found in biology. Although less common in biology, Ni(II) was screened and shown to elicit no fluorescence response from FerriBRIGHT. Biologically relevant ROS, such as H_2O_2, HO•,

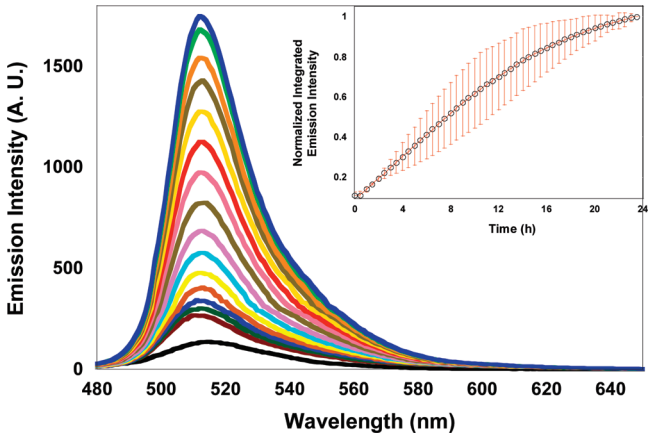

Figure 8. Oxidation of 1.6 μM FerriBRIGHT with 10 equiv of $[Co(NH_3)_5Cl]Cl_2$ in MeOH. The emission spectra were automatically recorded every 30 min for 24 h. Excitation was provided at 465 nm with an excitation slit width of 5.0 nm and emission slit width of 10.0 nm. Inset: changes in integrated fluorescence emission between 480 and 650 nm over 24 h with error bars corresponding to variations over three trials.

$O_2^{\bullet-}$, and $^1O_2$, were all exposed in excess to FerriBRIGHT, and little to no change in the emission intensity was observed. Likewise, other oxidants, such as *t*-BuO_2H (T-Hydro), $K_3Fe(CN)_6$, and commercial bleach (NaOCl) all failed to yield emission enhancements from FerriBRIGHT. From these observations, the requisite coordination of a redox-active metal ion to the catechol adds a modicum of analyte selectivity to this redox detection strategy. It appears that strong, noncoordinating oxidants, such as DDQ or CAN, which are biologically irrelevant, are the only other species that afford the desired emission enhancements. This selectivity in the signal transduction may help distinguish oxidative stress caused by ROS or adventitious copper and iron in the biological milieu.

Conclusion

A novel BODIPY−catechol dyad was designed by rational methods guided by computational methods. Isolation of the dipyrrin during the synthesis of FerriBRIGHT resulted in a significant improvement in the isolated yield of product over reported procedures for preparing BODIPY derivatives with carbonyl-containing substituents. We have also demonstrated the practical application of microwave-assisted hydrogenation to synthesis of the title molecule. FerriBRIGHT exhibits a significant increase in fluorescence upon the addition of redox-active metals that can coordinate to the pendant catechol and oxidize it to the corresponding quinone. This oxidation interrupts PeT by lowering the energy of the HOMO involved in fluorescence quenching. To our knowledge, this is only the second example of a probe that utilizes metal-based oxidation of a PeT quencher to elicit a positive fluorescence response. A copper chemidosimeter that relies on phenothiazine oxidation was recently reported.[42] The catechol ring is selectively oxidized with Fe(III), Cu(II), Co(III), DDQ, and CAN, which results in large changes of the emission intensity of the BODIPY fluorophore, whereas the reactive oxygen species do not drastically change the fluorescence properties of FerriBRIGHT. This unique strategy for combining coordination and oxidation may serve as a useful strategy for designing fluorescence probes for biologically relevant redox-active metal ions. Investigations are under way aimed at improving the water solubility and analyte selectivity of the system. The development of these new tools should complement the emerging numbers of fluorescent probes designed to image oxidants such as H_2O_2, O_2^-, and $^1O_2$ and other species that do not respond specifically to metal oxidation pathways.

Acknowledgment. This work was supported by the University of Connecticut and University of Connecticut Research Foundation Fund 1171. We thank Professor Nicholas Leadbeater for use of his microwave instrument for hydrogenation reactions. We thank Professor Jose Gascon for assistance with Gaussian. We thank Yu Shi and Professor Xudong Yao for assistance acquiring the HRMS data for both quinone compounds.

Supporting Information Available: ^1H and ^{13}C NMR spectra for all documented compounds, full citation for refs 26 and 28, Figure S1 showing the overlay of the ^1H NMR from the aromatic region of FerriBRIGHT and FerriBRIGHT-Q, Figure S2 showing the response of FerriBRIGHT-Q to added sodium ascorbate, Figure S3 showing the difference spectrum for the absorbance used in Job's analysis of FerriBRIGHT and Ga^{3+}, and Figure S4 showing the Hill plot from the titration of FerriBRIGHT with Ga^{3+}. This information is available free of charge via the Internet at http://pubs.acs.org.

JA901653U

(42) Ajayakumar, G.; Sreenath, K.; Gopidas, K. R. *Dalton Trans.* **2009**, 1180–1186.